

# Room-Temperature Number-Resolving Single-Photon Detection by SOI MOSFET

Wei Du, Hiroshi Inokawa and Hiroaki Satoh

Research Institute of Electronics, Shizuoka University

3-5-1 Johoku, Naka-ku, Hamamatsu 432-8011, Japan, Phone: +81-53-478-1325 E-mail: duwei@rie.shizuoka.ac.jp

## 1. Introduction

Conventional single-photon detectors, such as photomultiplier tubes and avalanche photo diodes, rely on carrier multiplication, and suffer from timing jitter, gain fluctuation, dark counts, afterpulsing, etc. In order to solve these, detectors are anticipated, which can directly count photo-generated carriers one by one without multiplication. Such detectors are also expected to have photon-number resolution that is useful in some classes of quantum key distribution [1] and quantum computation [2].

In this report, photo-response of the scaled-down silicon-on-insulator (SOI) metal-oxide-semiconductor field-effect transistor (MOSFET) [3] is investigated precisely, which has a charge sensitivity of single-electron resolution, and can be a multiplication-free single-photon detector by utilizing the internal separation of photo-generated carriers (electrons and holes).

## 2. Experimental Methods

Figure 1 shows (a) the top and (b) cross-sectional views of the device. In this structure, photo-generated holes can be trapped under the lower gate (LG) when negative voltage ( $V_{LG} < 0$ ) is applied, whereas back electron channel, which is used as electrometer, can be formed with positive substrate voltage ( $V_{SUB} > 0$ ). Photo-generation of holes and their recombination will modulate the electron current, and can be detected as pulses.

Two devices listed in Table I are evaluated. #1 shows lower dark counts and is measured at 300K, and #2 at 250K, where dark counts are negligible. It seems that the difference is individual and is not related  $L$ ,  $W$  or number of LG.

## 3. Results and Discussion

Figure 2 shows drain current waveforms for different level of incident light intensities at wavelength of 550nm for device #1 at 300K. We shift each waveform for clarity. It shows that pulse count increases as photon incident rate increases. Moreover, different pulse levels can be seen clearly, suggesting different number of holes trapped under the lower gate. The 1st, 2nd, 3rd and 4th levels correspond to number of trapped holes of 0, 1, 2 and 3, respectively. There is proportionality between count rate and photon incident rate, as shown in Fig. 3. This relationship indirectly proves that the obtained pulse correspond to single photons. Figure 3 also shows the wavelength dependence of device #2 at 250K. Figure 4 shows quantum efficiency (QE) as a function of wavelength derived from Fig. 3 for both devices #1 and #2. Light absorption by 50-nm thick Si slab is nearly parallel to the experimental data, indicating

that the spectroscopic behavior of QE is mainly governed by the Si absorption coefficient. The low QE results from the upper gate covering the active (undoped) Si area, and can be improved by removing the upper gate, although adjustment of bias voltages and channel dopant concentration is necessary.

Figure 5 (a)-(e) are histograms of drain currents corresponding to Fig. 2. The solid points are obtained data and red lines are fitting curves with Gaussian distribution. The peaks correspond to the number of trapped holes of 0, 1, 2 and 3, from the left. When incident light intensity increases, more and more holes are generated, thus possibility of holes being trapped increases, resulting in the higher peaks for more trapped holes. Figure 6 shows probability of each state corresponding to the number of trapped holes, as a function of generation rate. The theoretical curves (red lines) are obtained from rate equations and hole lifetimes of 11, 5 and 1 ms for the trapped holes of 1, 2 and 3, respectively. Experimental data (solid points) and theoretical ones coincide well, suggesting that the photon number can be resolved up to three with time resolution smaller than 1 ms.

Figure 7 shows recombination rate of holes as a function of drain current for different numbers of trapped holes  $n_h$ . Recombination rate vs. current follows the power law with an exponent of 0.42, and almost proportional to the number of trapped holes. These behaviors indicate that recombination is not a simple bimolecular process, as opposed to [3]. Contribution of indirect process (e.g. via recombination center) is a possibility.

## 4. Conclusions

SOI MOSFET was evaluated as a single-photon detector. Some device showed dark counts less than  $0.02 \text{ s}^{-1}$  even at 300 K, and the output waveforms exhibited clear separation of current levels corresponding to different numbers of photo-generated and trapped holes, indicating the possibility of photon-number resolution. The recombination mechanism of the holes was also investigated, and indirect transition was suggested.

## Acknowledgements

Authors are deeply indebted to K. Yamada of Waseda University, T. Chikyo of National Institute of Materials and Science, T. Endoh of Tohoku University, H. Yoshino and S. Fujisawa of Semiconductor Leading Edge Technologies, Inc. for their cooperation in the device fabrication.

## References

- [1] N. Gisin et al., Rev. Mod. Phys. **74** (2002) 145.
- [2] E. Knill et al., Nature **409** (2001) 46.
- [3] A. Fujiwara et al., Appl. Phys. Lett. **80** (2002) 4567.

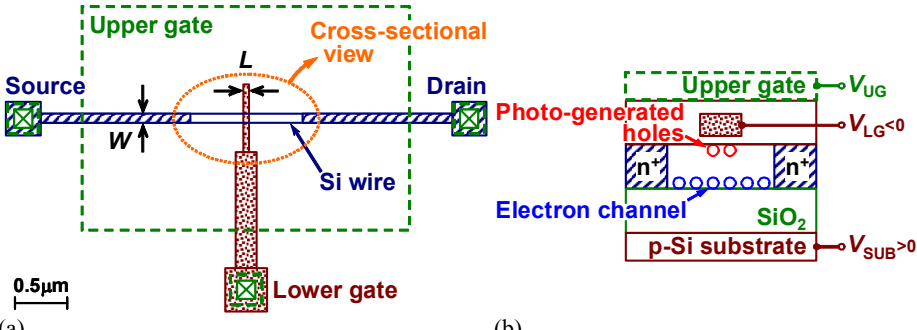


Fig. 1 Device structure. (a) Top view. (b) Cross-sectional view. Photo-generated holes are trapped below the lower gate with limited lifetime, and modulate the electron current. The thicknesses of buried oxide, SOI, LG oxide and insulator below the UG are 145, 50, 5 and 440 nm, respectively.

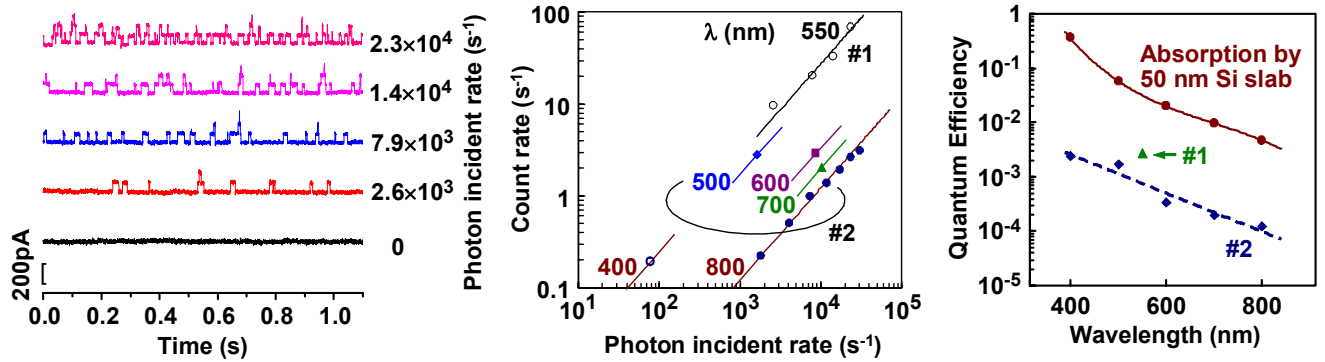


Fig. 2 Drain current waveforms for different level of light intensities for device #1 at 300 K. Each waveform is shifted for clarity.

Fig. 3 Pulse count rate (number of rising edges) vs. photon incident rate. Data for devices #1 and #2 are obtained at 300 and 250 K, respectively.

Table I List of devices. Device #1 has two lower gates (LG), but one of two LG's is disabled by high  $V_{LG}$ .

Device	#1	#2
Structure	2LG	1LG
L (nm)	65	70
W (nm)	105	110
Dark Count (s <sup>-1</sup> )		
300 K	< 0.02	1.4
250 K	---	< 0.01

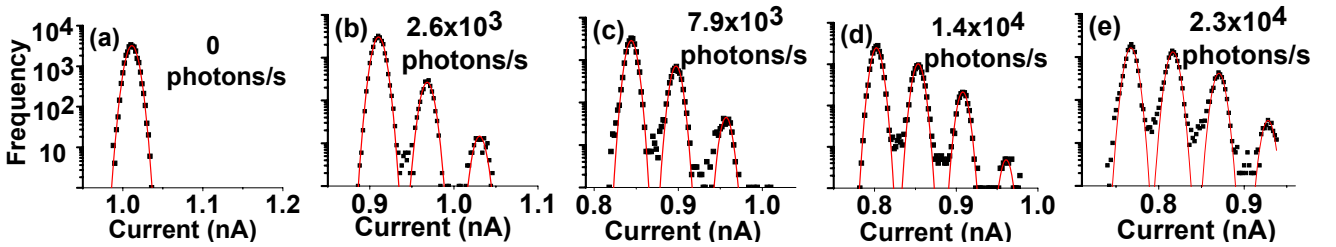


Fig. 5 Histograms of digitized drain currents corresponding to Fig. 2. 1st, 2nd, 3rd and 4th peaks correspond to the number of trapped holes of 0, 1, 2 and 3, respectively. Observation time and time step are 1.56 s and 61  $\mu$ s, respectively.

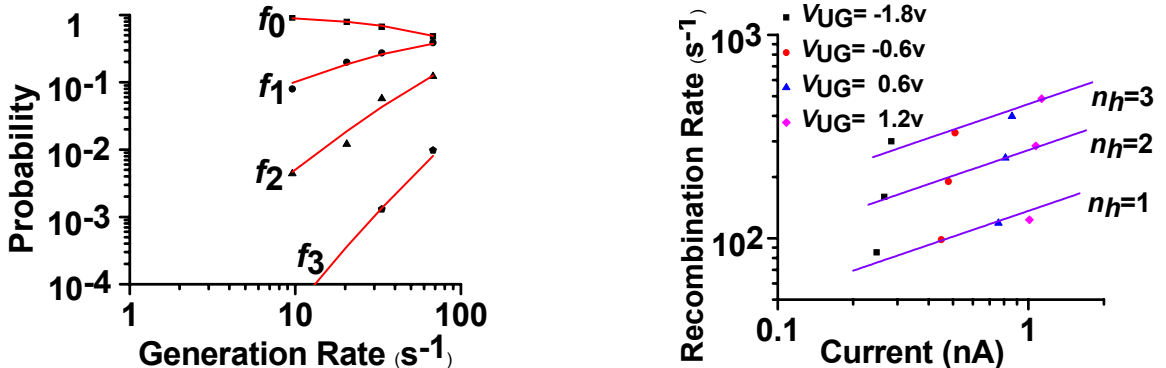


Fig. 6 Probability of states vs. photo-generation rate of holes obtained from Fig. 5. States  $f_0, f_1, f_2$  and  $f_3$  correspond to the number of trapped holes of 0, 1, 2 and 3, respectively.

Fig. 7 Recombination rate of holes vs. drain current for different number of trapped holes  $n_h$ . Drain current is adjusted by  $V_{UG}$ . Data are obtained from device #1 at 300 K.